Available online at www.sciencedirect.com
SCIENCE DIRECT
Tectonophysics 418 (2006) 21–30
TECTONOPHYSICS
www.elsevier.com/locate/tecto

High-field cantilever magnetometry as a tool for the determination of the magnetocrystalline anisotropy of single crystals

Fátima Martín-Hernández [a,*], Iris M. Bominaar-Silkens [b,1], Mark J. Dekkers [a,2], Jan Kees Maan [b,1]

[a] *Paleomagnetic Laboratory "Fort Hoofddijk", Faculty of Geosciences, Utrecht University, Budapestlaan 17, 3584 CD Utrecht, The Netherlands*
[b] *High Field Magnet Laboratory, Institute for Molecules and Materials, Radboud University Nijmegen, Toernooiveld 7, 6525 ED Nijmegen, The Netherlands*

Received 1 April 2005; received in revised form 18 October 2005; accepted 5 December 2005
Available online 28 February 2006

Abstract

Cantilever torque magnetometry is utilized widely in physics and material science for the determination of magnetic properties of thin films and semiconductors. Here, we report on its first application in rock magnetism, namely the determination of K_1 and K_2 of single crystal octahedra of natural magnetite. The design of cantilever magnetometers allows optimization for the specific research question at hand. For the present study, a cantilever magnetometer was used that enables measurement of samples with a volume up to 64 mm^3. It can be inserted into an electromagnet with a maximum field of 2 T. The cantilever spring is suitable for torque values ranging from 7.5×10^{-7} N·m to 5×10^{-6} N·m. The torque is detected capacitively; the measured capacitance is converted into torque by using a calibrated feedback coil. The magnetometer allows in-situ rotation of the sample in both directions and is, therefore, also suitable to analyze rotational hysteresis effects.

The evaluation of the magnetite anisotropy constants involved Fourier analysis of the torque signal on the magnetite crystals' (001) and (110) planes. The absolute anisotropy constant has been computed using the extrapolation-to-infinite-field method. The value of K_1 at room temperature is determined at -1.28×10^4 [J m^{-3}] (± 0.13, i.e. 10%) and that of K_2 at -2.8×10^3 [J m^{-3}] (± 0.1, i.e. 2%). These values concur with earlier determinations that could not provide an instrumental error, in contrast with this work.

The cantilever magnetometer performs four times faster than other torque magnetometers used for rock magnetic studies. This makes the instrument also suitable for magnetic fabric analysis.

Keywords: Magnetocrystalline anisotropy constants; Cantilever magnetometer; Magnetite; Rock magnetism

1. Introduction

Magnetite is the most abundant magnetic mineral in terrestrial rocks and its magnetic properties have therefore been studied intensively (summarized in O'Reilly, 1984; Dunlop and Özdemir, 1997). It is a cubic mineral crystallizing in the spinel structure, with anisotropy constants at room temperature $K_1=-1.35\times10^4$ [J m^{-3}] and $K_2=-2.80\times10^3$ [J m^{-3}] (Syono, 1965). Despite the

* Corresponding author. Tel.: +31 30 2531361; fax: +31 30 2431667.
E-mail addresses: fatima@geo.uu.nl (F. Martín-Hernández), I.Bominaar@science.ru.nl (I.M. Bominaar-Silkens), dekkers@geo.uu.nl (M.J. Dekkers), JC.Maan@science.ru.nl (J.K. Maan).
[1] Tel.: +31 24 3652237; fax: +31 24 3652440.
[2] Tel.: +31 30 2531361; fax: +31 30 2431667.

0040-1951/$ - see front matter © 2006 Elsevier B.V. All rights reserved.
doi:10.1016/j.tecto.2005.12.011

importance of knowing these values as exact as possible for micromagnetic calculations (e.g., Enkin and Dunlop, 1987; Williams and Dunlop, 1989; Williams and Wright, 1998) or for theoretical models of first-order-reversal-curves (FORC) diagrams (Carvallo et al., 2003), K_1 has been evaluated only on a few occasions (Syono, 1965; Sawaoka and Kawai, 1967; Fletcher and O'Reilly, 1974; Kakol et al., 1991), while K_2 has been determined only twice (Bickford et al., 1957; Syono, 1965).

The most common technique to determine magnetic anisotropy constants is the torque magnetometer (Tarasov and Bitter, 1937; Burd et al., 1977; Huq and Lee, 1978). While AC bridge-type susceptometers are very precise for the determination of the anisotropy ellipsoids of the low-field or initial susceptibility, torque magnetometers can measure the anisotropy in much higher magnetic fields as well (up to a few Tesla). For rock samples, the anisotropy of the high field magnetic susceptibility in terms of directions and shape of the ellipsoid was calculated on basis of torque magnetometer data (Banerjee and Stacey, 1967; Parma, 1988; Bergmüller et al., 1994). Often the total fabric is composed of several subfabrics and Hrouda and Jelinek (1990) and Martín-Hernández and Hirt (2004) were able to compute the separate anisotropy tensors of paramagnetic and ferrimagnetic minerals by means of torque measurements in several fields. When ferrimagnetic minerals are measured in applied magnetic fields above saturation, the magnetic torque is constant with applied field, while for paramagnetic minerals the torque is proportional to the square of the field. These different field dependencies are used to separate the two anisotropy tensors. However, the torque magnetometers up to now are designed for standard paleomagnetic specimens (25.4 mm diameter and 22 mm height); they are less suited for a proper measurement on much smaller single crystals, being either synthetic or of natural origin.

Recently, sensitive microcantilever torque magnetometers have been developed to accurately evaluate the magnetic anisotropy in thin films and recording media (Löhndorf et al., 2000; Hopfl et al., 2001). They allow also the determination of rotational hysteresis, to estimate the degree of magnetic exchange interaction, being very effective in ferrimagnetic and antiferromagnetic phases (Yoshida et al., 1994; Koike et al., 1999; Vopsaroiu and Bissell, 2002). Here, we report on a cantilever magnetometer that operates in fields from 0 to 2 T and that can measure specimens with sizes up to $4\times4\times4$ mm^3, ideal for the determination of the anisotropy constants of natural ferromagnetic single crystals. Instrumental characteristics, drift and how to cope with it, limits of detection, performance in terms of measurement duration are described for five natural single crystals of magnetite. We confirm earlier measurements of K_1 and K_2 with experimental error never evaluated before. The potential for rock samples is discussed and full anisotropy evaluation of other natural magnetic minerals is envisaged in the future.

2. High-field cantilever magnetometer

In material sciences, cantilever torque magnetometers are relatively well known, most are so-called microcantilevers based on capacitive torque detection (Chaparala et al., 1992; Rossel et al., 1998). Such a cantilever is based on a capacitor with a certain interplate distance d (Fig. 1). The two plates are connected by a flexible membrane that allows variation of the distance between the two plates. This flexible tongue is connected to a fixed platform through a beam (Fig. 1b). The instrument has a feedback coil on top of the upper capacitor plate for calibration purposes. The coil is wound around a plastic cylinder on top of which the sample can be placed (Fig. 1b).

In the presence of a magnetic field, the magnetization of an anisotropic sample is not exactly parallel to the direction of the applied field, but it has an angle θ. The torque (**T**) exerted by a magnetic moment in the presence of a magnetic field is given by:

$$\mathbf{T} = \mathbf{m} \times \mathbf{B} \tag{1}$$

where **m** is the magnetization and **B** is the applied magnetic field. The direction of the torque is always perpendicular to the plane defined by **m** and **B**, and therefore it is a vector perpendicular to the frontal view shown in Fig. 1a. The effect of the torque is a change in the distance d between the two capacitor plates, which causes a variation in the capacitance.

A rotating wheel allows the cantilever to vary its orientation with respect to the direction of the applied field. A stepper motor is connected to the cantilever, which is operated by a personal computer. The capacitance, which is proportional to the torque, is evaluated as a function of angle. The whole cantilever set-up is placed between the poles of an electromagnet that can generate fields up to 2 T. The capacitance is read by an ultra-precision capacitance bridge model 2500A 1 kHz, manufactured by "Andeen Hagerling".

It is transformed into torque through the calibration coefficient determined with the feedback coil mounted on top of the upper capacitor plate (Fig. 1a), a method often used to calibrate torque magnetometers (Pearson, 1979). The current through the coil (3.5 mm in diameter

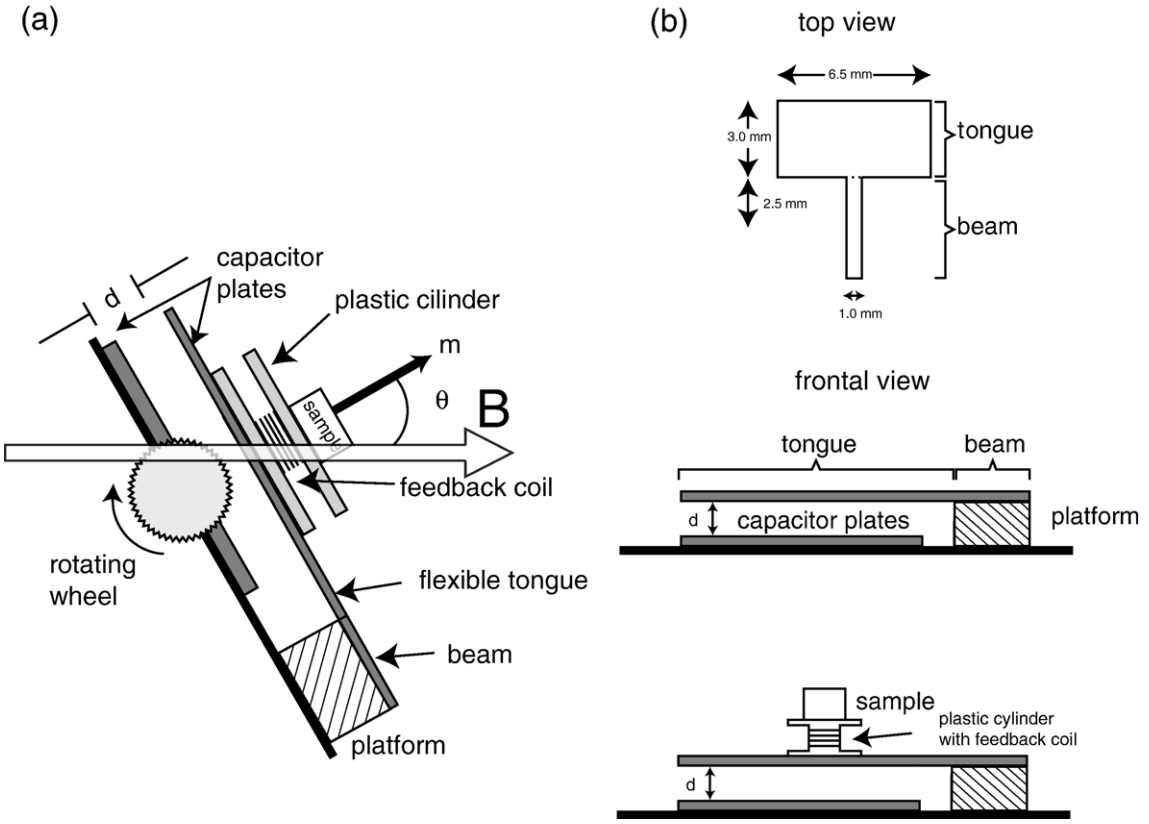

Fig. 1. Schematic drawing of the cantilever. (a) Lateral view of the cantilever showing the two plates that constitute the capacitor and their initial distance, the location of the calibrating feedback coil, flexible tongue and rotating wheel. (b) Detailed drawing of the location of the tongue and beam from top (above) and a lateral view (below). Lower most drawing shows the location of the sample on top of the feedback coil.

with 10 turns) can be changed; therefore it is possible to create a varying magnetization in the direction perpendicular to the coil plane. Its magnitude is $m=nAi$ with m is the magnetization, n is the number of turns, A is the area of the coil and i is the electric current in A. The feedback is used for the calibration of the instrument. For several currents in the coil torque T is calculated and with the corresponding measured capacitance the calibration constant is determined (Fig. 2a).

The feedback coil also allows the determination of the detection limit of the instrument. The coil is oriented 90° with respect to an applied field of 1.5 T. By changing the direction and amount of current through the feedback coil (steps of 10 mA, 5 mA, −5 mA and

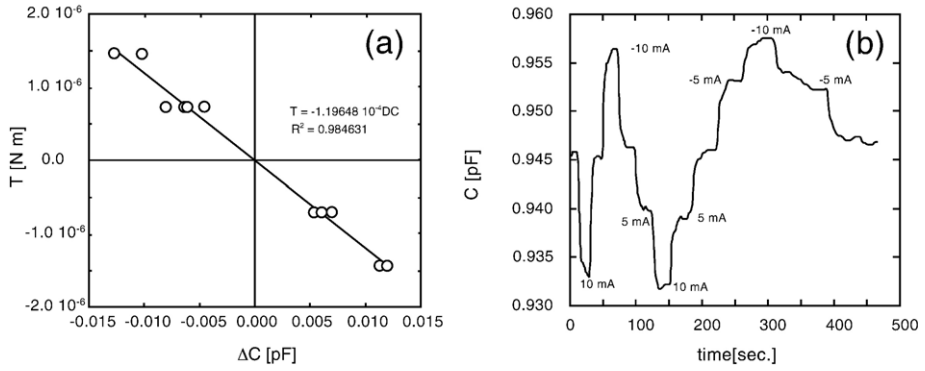

Fig. 2. (a) Capacitance measured while varying the applied current in a step-like manner. The magnetic field of 1.5 T is oriented perpendicular to the plane of the current coil. (b) Capacitance measured as a function of time for different currents through the feed-back coil.

−10 mA) it was established that 5 mA could be resolved (Fig. 2b). Using Eq. (1) the estimated minimum sensitivity is 5×10^{-7} Am^2.

3. Description and rock magnetic properties of the samples

The analyzed samples are natural octahedral magnetite single crystals from a greenschist from Green Mill (Maryland, USA). Samples of approximately 8 mm^3 have been selected because this is most suited for the cantilever. To determine the purity and domain state of the magnetite several rock magnetic experiments have been carried out.

The chemical composition is (values in g/kg) 680.5 Fe, 0.55 Al, 0.60 Ca, 0.05 K, 0.45 Mg, 0.85 Mn, 1.60 Ti (Franke et al., in preparation) corresponding to 0.67% non-Fe cations.

The Curie temperature was measured in air on a modified translation Curie balance (Mullender et al., 1993). The so-called incremental heating and cooling segments protocol was used to detect chemical alteration; the final heating temperature was 650°C. The Curie temperature, determined by "intersecting tangent" method (Grommé et al., 1969; Moskowitz, 1981), is 578±2 °C (Fig. 3a) indicative of pure magnetite (e.g., Dunlop and Özdemir, 1997). The 2nd derivative method (Tauxe, 1998) yielded the same estimate (within error margin) of 577 °C.

Hysteresis loops were measured on an alternating gradient magnetometer (Princeton Inc. Micromag 2900 model) to determine the saturation magnetization (M_s), remanent saturation (M_{rs}), and coercive force (B_c). As anticipated, the measurements show an almost closed loop, representative for the multidomain state. Saturation magnetization is about 89 Am^2/kg achieved in a field of about 250 mT, another indication of pure magnetite.

First-order reversal curve (FORC) diagrams were measured to determine the domain state and microcoercivity spectrum (Roberts et al., 2000; Pike et al., 2001). The diagram shows slightly asymmetrical

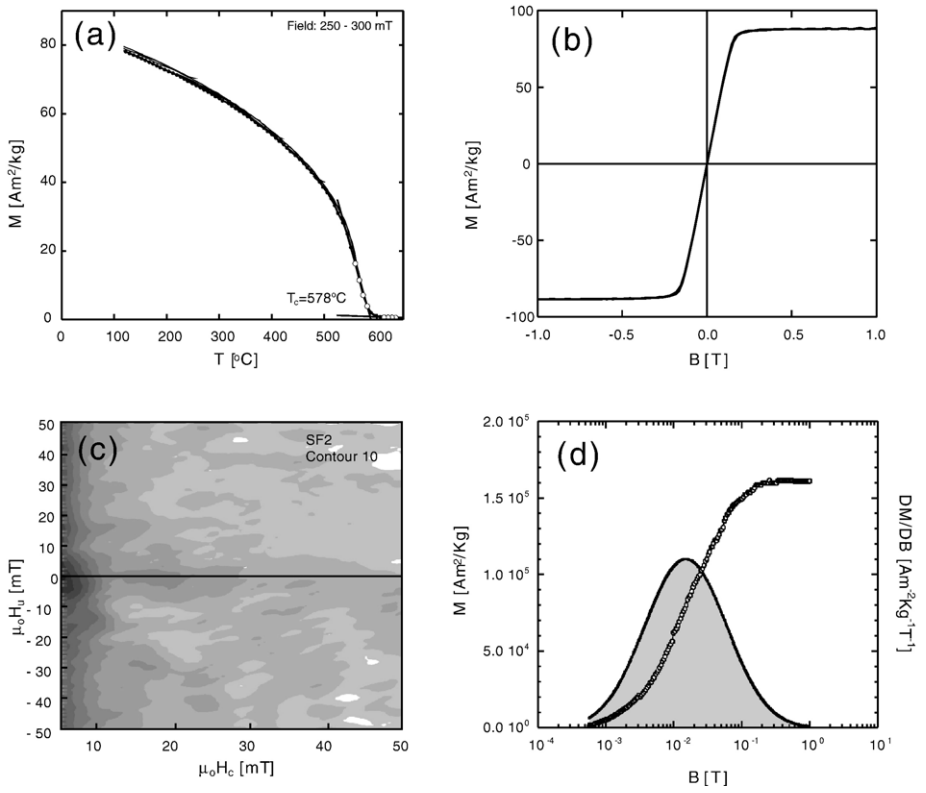

Fig. 3. Rock magnetic experiments on octahedral magnetite single crystals. (a) Determination of the Curie temperature with a modified horizontal translation Curie balance with the applied field cycling between 150 and 300 mT. Open symbols represent the points used for the linear fitting in the determination of the Curie temperature, (b) major hysteresis loop, (c) FORC diagram with a smoothing factor SF=2 in contour intervals of 10 and (d) IRM acquisition curve and coercivity spectrum using software developed by Kruiver et al. (2001). The $B_{1/2}$ is 15.8 mT and the dispersion parameter of the fitting is DP=0.62.

vertical contour lines (Fig. 3c), indicative of multidomain particles. The asymmetry can be attributed to minor amount of stress accumulated within the magnetic crystal (Pike et al., 2001) although most of the FORC diagrams are asymmetric due to the intrinsic asymmetry of the measurements as it has been discussed by Muxworthy and Williams (2005).

Isothermal Remanent Magnetization (IRM) acquisition curves up to 2 T were acquired with the alternating gradient magnetometer as well. The curve shape and saturation field are used very often to identify magnetic minerals (e.g., Dunlop and Özdemir, 1997; Evans and Heller, 2003). The coercivity spectra give information on the number of coercivity populations in the sample as well as on their coercivity properties (Kruiver et al., 2001; Heslop et al., 2002; Egli, 2004). Here, the derivative of the IRM acquisition curve has been fitted to a log-Gaussian distribution following the procedure outlined by Kruiver et al. (2001). The analyzed samples show the presence of a very low coercivity phase that saturates at about 200 mT, with a medium acquisition field of 16 mT (Fig. 3d).

4. Cantilever measurements

Five octahedral magnetite single crystals have been measured. The samples have been attached to the cantilever with non-magnetic varnish (GE varnish) supplied by Oxford Instruments. There was at least 1 h between the mounting of the magnetite crystal and the actual measurement to get completely dried varnish ensuring optimal data quality. Samples were measured first in a counterclockwise and then in a clockwise sense of rotation in angular steps of 10°, in various magnetic fields ranging from 50 mT to 2 T. For each field value, the mean torque of the clockwise and counterclockwise measurement is computed in order to eliminate rotational hysteresis effects (Burd et al., 1977; Huq and Lee, 1978). In a saturating magnetic field, the angular dependence of the torque for a magnetite crystal oriented with the magnetization constrained to the (001) plane with the initial field position along the [100] direction, is as follows (Bozorth, 1936; Syono, 1965; Burd et al., 1977):

$$T_{(001)} = -\frac{K_1}{2}\sin(4\theta) \qquad (2)$$

where K_1 is the first magnetocrystalline constant for magnetite and θ is the orientation of the field with respect to the [100] axis. The value of the first magnetocrystalline anisotropy constant is derived from the coefficient of the Fourier analysis of the signal associated with the 4θ-term.

Analogously, when the magnetization is constrained to lie in the (110) plane with the initial direction of magnetization in the [001] direction, the magnetic torque in fields higher than saturation is (Bozorth, 1936; Syono, 1965; Burd et al., 1977):

$$T_{(110)} = \frac{K_1}{8}(-2\sin(2\theta) - 3\sin(4\theta)) + \frac{K_2}{64}(-\sin(2\theta) - 4\sin(4\theta) + 3\sin(6\theta)) \qquad (3)$$

where K_2 is the second magnetocrystalline anisotropy constant for magnetite. The value of the second magnetocrystalline anisotropy constant is calculated from the 6θ-term of the Fourier analysis of the signal.

If saturation is reached by the sample, the amplitude of the torque as a function of field must remain constant independent of the strength of the applied field. Theoretically, however, only at infinite fields the saturation magnetization aligns perfectly with the applied field (Burd et al., 1977; Huq and Lee, 1978). In order to calculate the theoretical magnetocrysalline anisotropy constant the "*extrapolation to infinite field*" method has been used (Burd et al., 1977). A package of Matlab subroutines has been developed to compute the anisotropy coefficients.

4.1. Torque measurements

The torques of the five magnetite single crystal samples have been measured as function of angle in the (001) and (110) planes. Measurements in the (001) plane are characterized by a dominant 4θ-term (Fig. 4a). Overlapping the pure 4θ-term there is a 2θ-term due to a slight misorientation of the sample with respect to the (001) plane. Fourier analysis of the signal for the different applied fields (Fig. 4b) indeed shows the dominance of the 4θ-term (approximately an 85% of the signal) and the presence of the 2θ-term (14.5% of the signal). The 6θ-term comprises less than a few percent of the total signal and is considered not significant. The Fourier coefficients show an increase of the intensity with the applied field up to 300 mT, when the sample reaches saturation. With increasing field, in the 4θ-term first an increase in the signal is observed followed by a further decrease until the signal reaches saturation.

Measurements in the (110) plane are characterized by the combination of several terms (Fig. 4c). The Fourier analysis reveals the presence of a significant 6θ-term, in agreement with the theoretical expression of the torque in the (110) plane (Eq. (3)).

The magnetocrystalline anisotropy constants for the five crystals are summarized in Table 1 and Fig. 5. The

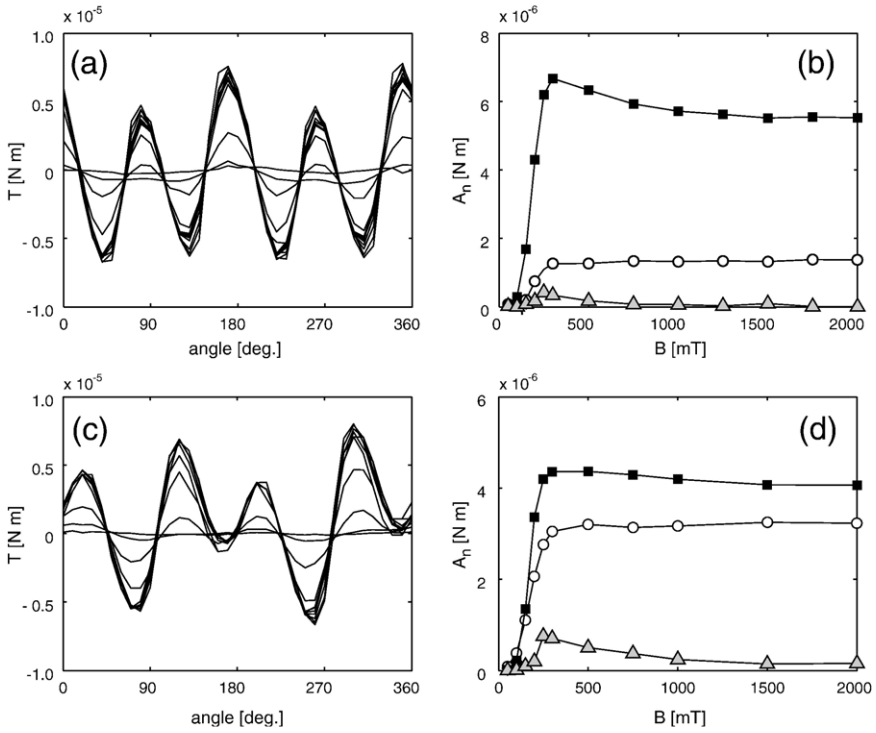

Fig. 4. Measured torque (T) for the magnetite single crystal mag.2 (left) and Fourier coefficients (A_n) of the torque signal where open circles represent the norm of the 2θ-term, full squares that of the 4θ-term and triangles that of the 6θ-term (right). The upper panels (a, b) show measurements on the (001) and the lower panels (c, d) show measurements on the (110) plane.

first anisotropy constant has been evaluated for the five crystals with the corresponding estimation of the error. A mean value of $K_1 = (-1.28 \pm 0.13) \times 10^4$ [J m^{-3}] was found. For the second anisotropy has also been evaluated in the five crystals. The error could not be determined in one of them, which was measured only at 2 T. A mean value of $K_2 = (-2.8 \pm 0.1) \times 10^3$ [J m^{-3}] was determined. The values of K_1 are more scattered than those of K_2. This is because the (001) plane of the samples is more difficult to orient than their (110) plane. The mean value of the obtained results is, within the calculated error, similar to the values reported by Syono (1965) and Sawaoka and Kawai (1967). It should be mentioned that values reported in this work are the only ones providing an estimate of the instrumental and measurement error. Anisotropy constants are utilized in a number of formulas. With the error estimate now available it can be assessed how this would propagate in parameters derived from the anisotropy constants.

4.2. Rotational hysteresis

Rotational hysteresis is the energy stored by a magnetic particle when it rotates in a magnetic field.

Table 1
Magnetocrystalline anisotropy constants computed for the analyzed octahedral magnetite single crystals with their mean value and values reported by Syono (1965)

Sample	Mass [gr.]	K_1 [J m^{-3}]	ΔK_1[J m^{-3}]	K_2[J m^{-3}]	ΔK_2[J m^{-3}]
mag.2	0.00665	-1.41×10^4	0.013×10^4	-2.79×10^3	0.555×10^3
mag.3	0.01645	-1.17×10^4	0.029×10^4	-2.77×10^3	1.408×10^3
mag.4	0.00549	-1.41×10^4	0.003×10^4	-2.77×10^3	1.109×10^3
mag.5	0.02053	-1.12×10^4	0.013×10^4	-2.76×10^3	~
mag.6	0.01150	-1.29×10^4	0.003×10^4	-2.92×10^3	0.533×10^3
Mean value		-1.28×10^4	0.13×10^4	-2.8×10^3	0.1×10^3
Syono (1965)		-1.35×10^4		-2.80×10^3	

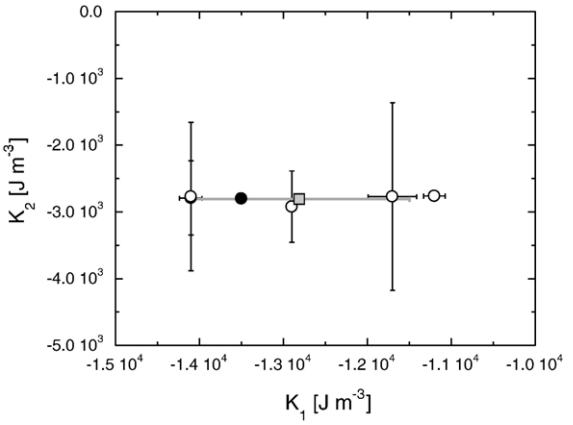

Fig. 5. Calculated values of the two magnetocrystalline anisotropy constants for magnetite (open circles). The error bars are computed from the estimated error based on predictions when representing the Fourier coefficients as a function of applied field. Full circle represents the mean value and the error bars are given by the standard deviation. Full square shows values reported by Syono (1965).

Irreversible magnetization processes only are sensed by rotational hysteresis. The energy increases with increasing applied field until it reaches a maximum related to the anisotropy constant and coercivity of the particles. Above this point it decreases to zero at a rate that depends on the magnetic particles, their domain state, oxidation, or orientation. It is not a very often used parameter; however it can provide useful information about the nature of the magnetic particles and the number of populations, their oxidation state, or the degree of exchange interaction between particles. In particular, core–rim interaction is one of the most difficult parameters to evaluate in rock magnetism but plays very important role in the remanence of sediments when magnetite particles are surrounded by an oxidized or partially maghemitized rim.

If the torque of an anisotropic specimen in a magnetic field is $T(\theta)$, the rotational hysteresis is computed as the integral over the full rotation (e.g., Bozorth, 1951; Collinson and Creer, 1960; Stacey and Banerjee, 1974).

$$W_R = \frac{1}{2\pi}\int_0^{2\pi} T(\theta)\mathrm{d}\theta \quad (4)$$

W_R is the rotational hysteresis in Joules, θ is the angle between the applied field and the origin of coordinates in radians, and T is the magnetic torque in N m.

Several theoretical models have been proposed to explain the variations of rotational hysteresis with applied field (Stoner and Wohlfarth, 1948; Owens, 1981). The general experimental feature that W_R displays is a peak related with the anisotropy constants (Owens, 1981). The position of the maximum value of W_R and its value has been used to identify magnetic phases in natural samples (Schmidbauer, 1988; Keller and Schmidbauer, 1996, 1999; Schmidbauer and Keller, 1996; Muxworthy et al., 2002). It has also been used to study the degree of oxidation of magnetic particles (Day et al., 1970).

The rotational hysteresis energy is computed as half of the area enclosed by the torque curve when the specimen is rotated twice, first in one sense of rotation and then in the opposite sense (Fig. 6a). The rotational hysteresis has been evaluated as a function of applied field for all the analyzed samples. It shows a maximum value, centered on approximately 150 mT. The peak of rotation hysteresis coincides with the expected values (Fig. 6b). The values are comparable with results reported previously for multidomain magnetite (Muxworthy, 2002). In fields above this maximum value, W_R values decay and tend to zero. The curve is narrower than earlier reported because the samples analyzed in this work are single crystals and samples previously analyzed consisted on non-oriented assemblages of

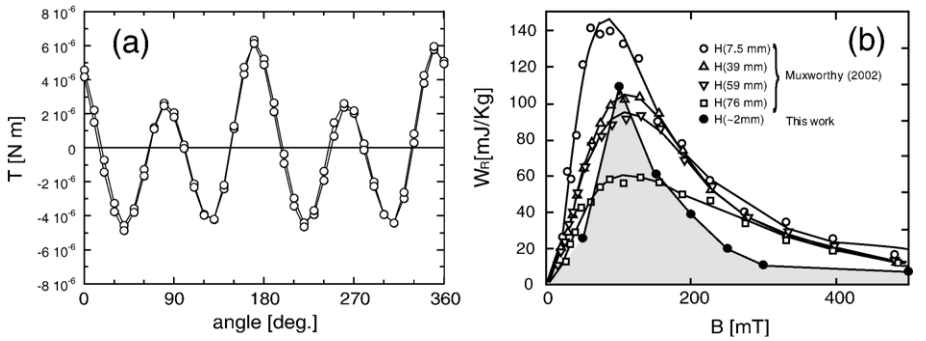

Fig. 6. Rotational hysteresis on a magnetite single crystal. (a) Rotational hysteresis is seen as the area (gray area) between the torque measured in the clockwise direction and the torque measured in the counterclockwise sense with an applied field of 150 mT. (b) Rotational hysteresis loss as a function of applied field (full symbols) compared with reported data (open symbols) (Muxworthy et al., 2002).

multidomain crystals (Elk, 1993). The rotational hysteresis can also be underestimated due to the measurement procedure. When the curves are measured the clockwise and counterclockwise curves coincide at 0° and 360°. To avoid this problem the curves are usually calculated through 540° between − 90° and 450° and only used the data from 0° to 360°. The device used here does not allow rotations of more than 360°. To avoid this problem the rotational hysteresis has been computed as twice the value between 90° and 270°.

5. Discussion

5.1. Magnetocrystalline anisotropy determinations

Strictly speaking, the constant determined by torque magnetometery is a combination of magnetocrystalline and magnetostriction constants (Ye et al., 1994). The magnetocrystalline anisotropy constant alone can be determined by ferromagnetic resonance, which has been evaluated for magnetite by Bickford (1949, 1950). For magnetite the magnetostriction term is small and it has been neglected by most studies (Syono, 1965; Kakol et al., 1991).

5.2. Instrument properties and performance

The measurement of a sample in the two senses of rotation takes about 20 min per applied field step. This may seem rather long, but nevertheless, the cantilever instrument is four times faster than other torque magnetometers available for rock magnetic fabrics (Bergmüller et al., 1994; Martín-Hernández and Hirt, 2001). So, the device allows a more precise evaluation of the desired parameters within the same time.

Samples with a combination of low-coercivity and high-coercivity minerals would need longer measuring time when the two subfabrics are separated. The presence of the latter makes it difficult to separate magnetic subfabrics due to the absence of saturation in the available magnetic fields (Martín-Hernández and Hirt, 2004). However this problem is not exclusive of this device but common to all torque magnetometers.

As with many instruments, cantilevers have a certain dynamic range. Samples with a very weak magnetization (e.g., weakly anisotropic paramagnetic samples or diamagnetic samples) are affected by the background signal. Samples with a very strong magnetization are out of the linear range between magnetization and capacitance and therefore not properly calibrated. A more robust feedback coil would be necessary in order to calibrate the instrument at higher magnetization ranges. The minimum detectable difference of magnetization estimated with the magnetization of the feedback coil is $\Delta m \sim 10^{-7}$ A m^2. The detectable range of differences in susceptibility estimated for a sample of 27 mm^3 is $\Delta K \sim 10^{-5}$ [S.I.].

5.3. Measurements

The measurements carried out are consistent with the theoretical expressions for the selected measuring planes (Fig. 4). An overlapping 2θ-term shows up in the measurements on the (001) plane which is supposed to be due to a small misorientation of the measuring plane (Fig. 4a). The 2θ-term has been attributed only to the magnetocrystalline anisotropy. In magnetite shape anisotropy is also important but for magnetite particles larger than 20 μm, shape anisotropy becomes less important (Dunlop and Özdemir, 1997). Due to the big size of the studied samples, this term has been neglected. The presence of this term might also be related with accumulation of strain due to the extraction process from the rock. Syono (1965) also reported a 2-θ-term in this measuring plane. Annealing might liberate the strain from the samples. Further work should be done to corroborate this hypothesis.

The two Fourier coefficients for the 4θ-term and 6θ-term display a similar behaviour, they increase until a maximum at the saturation field and followed by a decrease until a constant value is reached. Similar behaviour has been reported already in natural samples for the 4θ-term by Bergmüller and Heller (1996). It can be related with the asymptotic approximation of the magnetization to saturation.

6. Conclusion and perspective

Cantilever torque magnetometry has been revealed as an excellent tool also for rock magnetic analysis. The instrument allows measurement as a function of applied fields ranging from 0 to 2 T in the two senses of rotation. The minimum detectable difference of magnetization estimated with the magnetization of the feedback coil is $\Delta m \sim 10^{-7}$ A m^2. The detectable range of differences in susceptibility estimated for a sample of 27 mm^3 is $\Delta K \sim 10^{-5}$ [S.I.]. Cantilever magnetometers can be used for all utilities already set out for torque magnetometry applied to natural samples, e.g. separation of magnetic subfabrics (Hrouda and Jelinek, 1990; Martín-Hernández and Hirt, 2004). The instrument operates distinctly faster than classic torque magnetometers. It can be optimized for a specific dynamic range if desired. Because the two senses of rotation can be measured, it is also

possible to measure rotational hysteresis loss as a function of applied field. This would allow evaluation of magnetic interaction between the cores and oxidation rims of magnetic particles in rocks or the degree of interaction between particles of the same population (Muxworthy, 2001). Rotational hysteresis loss has been shown to be useful in rock magnetic studies, in particular to study the degree of oxidation in basalts (Day et al., 1970; Manson and O'Reilly, 1976; Schmidbauer and Keller, 1994), coercivity changes on heating (Cowan and O'Reilly, 1972) and coercivity of polluting particles (Muxworthy et al., 2002).

The anisotropy measurements carried out in the present study are consistent with the theoretical expressions for the selected measuring planes (Fig. 4). An overlapping 2θ-term shows up in the measurements on the (001) plane which is argued to be due to a small deviation of the measuring plane (Fig. 4a). The results obtained corroborate the values for $K_1 = -1.35 \times 10^4$ [J m^{-3}] and $K_2 = -2.80 \times 10^3$ [J m^{-3}] of magnetite that have been used in multiple applications such as micromagnetic calculations (Enkin and Dunlop, 1987; Carvallo et al., 2003; Muxworthy et al., 2004), analysis of coercivity properties (Ozdemir, 2000) or hysteresis simulations (Tauxe et al., 2002).

Acknowledgments

The authors would like to thank R. van Stijn (HFML) for his technical assistance and H. van Luong (HFML) for the development of the measuring software. Also thanks to M. Schaapman (HFML) for her useful comments at the beginning of this project. Comments by A. Muxworthy and an anonymous reviewer are gratefully thanked. This work has been supported by an EU Marie Curie Fellowship to FMH (project number MEIF-CT-2003-502133).

References

Banerjee, S.K., Stacey, F.D., 1967. The high-field torque-meter method of measuring magnetic anisotropy in rocks. In: Collinson, D.W., Creer, K.M., Runcorn, S.K. (Eds.), Methods in Palaeomagnetism. Elsevier, Amsterdam, pp. 470–476.

Bergmüller, F., Heller, F., 1996. The field dependence of magnetic anisotropy parameters derived from high-field torque measurements. Phys. Earth Plant. Inter. 96, 61–76.

Bergmüller, F., et al., 1994. A torque magnetometer for measurements of the high-field anisotropy of rocks and crystals. Meas. Sci. Technol. 5, 1466–1470.

Bickford Jr., L.R., 1949. Ferromagnetic resonance absorption magnetite. Phys. Rev. 76 (1), 137–138.

Bickford Jr., L.R., 1950. Ferromagnetic resonance absorption in magnetite single crystals. Phys. Rev. 78 (4), 449–457.

Bickford Jr., L.R., Brownlow, J.M., Penoyer, R.F., 1957. Magneto-crystalline anisotropy in cobalt-substituted magnetite single crystals. I.E.E.E., pp. 238–244.

Bozorth, R.M., 1936. Determination of ferromagnetic anisotropy in single crystals and in polycrystalline sheets. Phys. Rev. 50, 1076–1981.

Bozorth, R.M., 1951. Ferromagnetism. Van Nostrand, Princeton. 968 pp.

Burd, J., Huq, M., Lee, E.W., 1977. The determination of magnetic anisotropy constants from torque curves. J. Magn. Magn. Mater. 5 (2), 135–141.

Carvallo, C., Muxworthy, A.R., Dunlop, D.J., Williams, W., 2003. Micromagnetic modeling of first-order reversal curve (FORC) diagrams for single-domain and pseudo-single-domain magnetite. Earth Planet. Sci. Lett. 213 (3–4), 375–390.

Chaparala, M., Chung, O.H., Naughton, M.J., 1992. Capacitance platform magnetometer for thin film and small crystal supoerconductor studies. AIP, pp. 407–413.

Collinson, D.W., Creer, K.M., 1960. Measurements in palaeomagnetism. In: Runcorn, S.K. (Ed.), Methods and Techniques in Geophysics. Interscience Publishers, Inc., New York, pp. 168–210.

Cowan, B.K., O'Reilly, W., 1972. The effect of heat treatment on magnetic minerals in red sandstones, studied using the technique of rotational hysteresis. Geophys. J. R. Astron. Soc. 29, 263–274.

Day, R., O'Reilly, W., Banerjee, S.K., 1970. Rotational hysteresis study of oxidized basalts. J. Geophys. Res. 75, 375–386.

Dunlop, D.J., Özdemir, Ö., 1997. Rock Magnetism. Cambridge Univ. Press, Cambridge. 573 pp.

Egli, R., 2004. Characterization of individual rock magnetic components by analysis of remanence curves: 2. Fundamental properties of coercivity distributions. Phys. Chem. Earth 29 (13–14), 851–867.

Elk, K., 1993. Rotational hysteresis of polycrystalline permanent magnets. J. Magn. Magn. Mater. 123 (1–2), 117–125.

Enkin, R.J., Dunlop, D.J., 1987. A micromagnetic study of pseudo-single-domain remanence in magnetite. J. Geophys. Res. 92, 12726–12740.

Evans, M.E., Heller, F., 2003. Environmental Magnetism: Principles and Applications of Enviromagnetics. International Geophysics Series, vol. 86. Academic Press, London. 299 pp.

Fletcher, E.J., O'Reilly, W., 1974. Contribution of Fe^{2+} ions to the magnetocrystalline anisotropy constant K_1 of $Fe_{3-x}Ti_xO_4$ ($0<x<0.1$). J. Phys. C. Solid State Phys. 7, 171–178.

Franke C., Pennock G.M, Drury M.R., Engelmann R., Garming J.F.L., von Dobeneck T., Dekkers M.J., in preparation. Identification and characterisation of magnetic Fe–Ti-oxides by electron backscatter diffraction (EBSD) in scanning electron microscopy. Geophys. J. Int.

Grommé, S., Wright, T.L., Peck, D.L., 1969. Magnetic properties and oxidation of iron-titanium oxide minerals in Alae and Makaopuhi lava lakes, Hawaii. J. Geophys. Res. 74, 5277–5294.

Heslop, D., Dekkers, M.J., Kruiver, P.P., van Oorschot, I.H.M., 2002. Analysis of isothermal remanent magnetization acquisition curves using the expectation-maximazation algorithm. Geophys. J. Int. 148, 58–64.

Hopfl, T., Sander, D., Hoche, H., Kirschner, J., 2001. Ultrahigh vacuum cantilever magnetometry with standard size single crystal substrates. Rev. Sci. Instrum. 72 (2), 1495–1501.

Hrouda, F., Jelinek, V., 1990. Resolution of ferrimagnetic and paramagnetic anisotropies in rocks, using combined low-field and high-field measurements. Geophys. J. Int. 103, 75–84.

Huq, M., Lee, E.W., 1978. The determination of anisotropy constants from torque curves-II. J. Magn. Magn. Mater. 9 (4), 333–335.

Kakol, Z., Sabol, J., Honig, J.M., 1991. Magnetic anisotropy of titanomagnetites $Fe_{3-x}Ti_xO_4$, $0 < x < 0.55$. Phys. Rev., B 44, 2198–2204.

Keller, R., Schmidbauer, E., 1996. Rotational hysteresis losses of 10 nm γ-Fe_2O_3 particles at 130 K of water-based ferrofluid and of particles produced by bacteria. J. Magn. Magn. Mater. 162, 327–330.

Keller, R., Schmidbauer, E., 1999. Magnetic hysteresis properties and rotational hysteresis losses of synthetic stress-controlled titanomagnetite (Fe2.4Ti0.6O4) particles: II. Rotational hysteresis losses. Geophys. J. Int. 138 (2), 334–342.

Koike, I., Koga, S., Yamaguchi, T., 1999. Torque analysis of Co–Cr films prepared under different Ar pressures. IEEE Trans. Magn. 35 (5), 3022–3024.

Kruiver, P.P., Dekkers, M.J., Heslop, D., 2001. Quantification of magnetic coercivity components by the analysis of acquisition curves of isothermal remanent magnetisation. Earth Plant. Sci. Lett. 189 (3–4), 269–276.

Löhndorf, M., Moreland, J., Kabos, P., Rizzo, N., 2000. Micro-cantilever torque magnetometry of thin magnetic films. J. Appl. Phys. 87 (9), 5995.

Manson, A.J., O'Reilly, W., 1976. Submicroscopic texture in titanomagnetite grains in basalt studied using the torque magnetometer and electron microscope. Phys. Earth Plantet. Inter. 11, 173–183.

Martín-Hernández, F., Hirt, A.M., 2001. Separation of ferrimagnetic and paramagnetic anisotropies using a high-field torsion magnetometer. Tectonophysics 337, 209–221.

Martín-Hernández, F., Hirt, A.M., 2004. A method for the separation of paramagnetic, ferrimagnetic and hematite magnetic subfabrics using high-field torque magnetometer. Geophys. J. Int. 157 (1), 117–127.

Moskowitz, B.M., 1981. Methods for estimating Curie temperatures of titanomaghemites from experimental Js-T data. Earth Planet. Sci. Lett. 53, 84–88.

Mullender, T.A.T., van Velzen, A.J., Dekkers, M.J., 1993. Continuous drift correction and separate identification of ferrimagnetic and paramagnetic contributions in thermomagnetic runs. Geophys. J. Int. 114, 663–672.

Muxworthy, A.R., 2001. Introduction to rotational hysteresis and its potential use in enviromental magnetism. MAGazine 5–6.

Muxworthy, A.R., 2002. Magnetic hysteresis and rotational hysteresis properties of hydrotermally grown multidomain magnetite. Geophys. J. Int. 149 (3), 805–814.

Muxworthy, A., Williams, W., 2005. Magnetostatic interaction fields in first-order reversal curve (FORC) diagrams. J. Appl. Phys. 97, 063905.

Muxworthy, A.R., Schmidbauer, E., Petersen, N., 2002. Magnetic properties and Mossbauer spectra of urban atmospheric particulate matter: a case study from Munich, Germany. Geophys. J. Int. 150 (2), 558–570.

Muxworthy, A., Heslop, D., Williams, W., 2004. Influence of magnetostatic interactions on first-order-reversal-curve (FORC) diagrams: a micromagnetic approach. Geophys. J. Int. 158 (3), 888–897.

O'Reilly, W., 1984. Rock and Mineral Magnetism. Blackie, Glasgow. 230 pp.

Owens, W.H., 1981. A simple model for non-vanishing rotational hysteresis in haematite. Phys. Earth Plantet. Int. 27, 106–113.

Ozdemir, O., 2000. Coercive force of single crystals of magnetite at low temperatures. Geophys. J. Int. 141 (2), 351–356.

Parma, J., 1988. An automated torque meter for rapid measurement of high field magnetic anisotropy of rocks. Phys. Earth Planet. Inter. 51, 387–389.

Pearson, R.F., 1979. Magnetic anisotropy. In: Kalvius, G.M., Tebble, R.S. (Eds.), Experimental Magnetism. Willey, Chichester, pp. 137–223.

Pike, C.R., Roberts, A.P., Dekkers, M.J., Verosub, K.L., 2001. An investigation of multi-domain hysteresis mechanisms using FORC diagrams. Phys. Earth Plantet. Inter. 126 (1–2), 11–25.

Roberts, A.P., Pike, C.R., Verosub, K.L., 2000. First-order reversal curve diagrams: a new tool for characterising the magnetic properties of natural samples. J. Geophys. Res. 102, 28461–28475.

Rossel, C., et al., 1998. Torsion cantilever as magnetic torque sensor. Rev. Sci. Instrum. 69 (9), 3199–3203.

Sawaoka, A., Kawai, N., 1967. Change of magnetic anisotropy constant K1 of magnetite (Fe3O4) under hydrostatic pressure. Phys. Lett., A 24 (10), 503–504.

Schmidbauer, E., 1988. Magnetic rotational hysteresis study of spherical 85–160 nm Fe_3O_4 particles. Gephys. Res. Lett. 15 (5), 522–525.

Schmidbauer, E., Keller, R., 1994. Magnetic properties and rotational hysteresis of a basalt with homogeneous Ti-rich titanomagnetite grains 10–20 μm in diameter. Geophys. J. Int. 119, 880–892.

Schmidbauer, E., Keller, R., 1996. Magnetic properties and rotational hysteresis of Fe_3O_4 and gamma-Fe_2O_3 particles 250 nm in diameter. J. Magn. Magn. Mater. 152, 99–108.

Stacey, F.D., Banerjee, S.K., 1974. The Physical Principles of Rock Magnetism. Elsevier, Amsterdam. 195 pp.

Stoner, E.C., Wohlfarth, E.P., 1948. A mechanism of magnetic hysteresis in heterogeneous alloys. Philos. Trans. R. Soc. 240, 599–602.

Syono, Y., 1965. Magnetocrystalline anisotropy and magnetostriction of Fe_3O_4–Fe_2TiO_4 series, with special application to rock magnetism. Jpn. J. Geophys. 4, 71–143.

Tarasov, L.P., Bitter, F., 1937. Precise magnetic torque measurements on single crystals of iron. Phys. Rev. 52, 353–360.

Tauxe, L., 1998. Paleomagnetic Principles and Practice. Modern Approaches in Geophysics, vol. 17. Kluwer Academic Publishers, Dordrecht. 297 pp.

Tauxe, L., Bertram, H.N., Seberino, C., 2002. Physical interpretation of hysteresis loops: micromagnetic modeling of fine particle magnetite. Geochem. Geophy. Geosy. (Art. No. 1055).

Vopsaroiu, M., Bissell, P.R., 2002. Interaction effects on the anisotropy field in sputtered Co–Cr–Ta thin films and metal particle tapes. J. Phys., D, Appl. Phys. 35 (12), 1296–1300.

Williams, W., Dunlop, D.J., 1989. Three-dimensional micromagnetic modelling of ferromagnetic domain structure. Nature 337, 634–637.

Williams, W., Wright, T.M., 1998. High-resolution micromagnetic models of fine grains of magnetite. J. Geophys. Res. 103 (B12), 30537–30550.

Ye, J., Newell, A.J., Merrill, R.T., 1994. A re-evaluation of magnetocrystalline anisotropy and magnetostriction constants. Gephys. Res. Lett. 21, 25–28.

Yoshida, Y., Templeton, T.L., Arrott, A.S., 1994. Model-calculations of rotational hysteresis for ferromagnetic particles with competing anisotropies. J. Appl. Phys. 75 (10), 5695–5697.